Stroke

BASIC AND TRANSITIONAL SCIENCES

Bioresorbable Poly (L-Lactic Acid) Flow Diverter Versus Cobalt-Chromium Flow Diverter: In Vitro and In Vivo Analysis

Natsuhi Sasaki, MD; Akira Ishii, MD, PhD; Shinichi Yagi, PhD; Hidehisa Nishi, MD, PhD; Ryo Akiyama, MD; Masakazu Okawa, MD, PhD; Yu Abekura, MD, PhD; Hirofumi Tsuji, MD; Shinichi Sakurai, PhD; Susumu Miyamoto, MD, PhD

BACKGROUND: Permanent metallic flow diverter (FD) implantation for treatment of intracranial aneurysms requires antiplatelet therapy for an unclear duration and restricts postprocedural endovascular access. Bioresorbable FDs are being developed as a solution to these issues, but the biological reactions and phenomena induced by bioresorbable FDs have not been compared with those of metallic FDs.

METHODS: We have developed a bioresorbable poly (L-lactic acid) FD (PLLA-FD) and compared it with an FD composed of cobalt-chromium and platinum-tungsten (CoCr-FD). FD mechanical performance and in vitro degradation of the PLLA-FD were evaluated. For in vivo testing in a rabbit aneurysm model, FDs were implanted at the aneurysm site and the abdominal aorta in the PLLA-FD group (n=21) and CoCr-FD group (n=15). Aneurysm occlusion rate, branch patency, and thrombus formation within the FD were evaluated at 3, 6, and 12 months. Local inflammation and neointima structure were also evaluated.

RESULTS: Mean strut, porosity, and pore density for the PLLA-FD were 41.7 μm, 60%, and 20 pores per mm^2, respectively. The proportion of aneurysms exhibiting a neck remnant or complete occlusion did not significantly differ between the groups; however, the complete occlusion rate was significantly higher in the PLLA-FD group (48% versus 13%; P=0.0399). Branch occlusion and thrombus formation within the FD were not observed in either group. In the PLLA-FD group, CD68 immunoreactivity was significantly higher, but neointimal thickness decreased over time and did not significantly differ from that of the CoCr-FD at 12 months. Collagen fibers significantly predominated over elastic fibers in the neointima in the PLLA-FD group. The opposite was observed in the CoCr-FD group.

CONCLUSIONS: The PLLA-FD was as effective as the CoCr-FD in this study and is feasible for aneurysm treatment. No morphological or pathological problems were observed with PLLA-FD over a 1-year period.

GRAPHIC ABSTRACT: A graphic abstract is available for this article.

Key Words: absorbable implants ■ animal experiments ■ intracranial aneurysm ■ polymers ■ stent

The effectiveness of flow diverter (FD) treatment of intracranial aneurysms has been demonstrated in numerous studies.[1–4] The complete aneurysm occlusion rate at a 1-year follow-up was 81.9% with Pipeline (Medtronic) and 95.3% with FRED (Microvention, Aliso Viejo, CA), which is structurally different from Pipeline.[4,5] Diversion of blood flow by FD enables thrombus formation within the aneurysm sac. Moreover, endothelial cells grow along the FD scaffold. These phenomena can result in aneurysm occlusion and prevent a recurrence.[6] In view of its efficacy and healing mechanism, the braided stent design with its dense weave and small pores may

Correspondence to: Akira Ishii, MD, PhD, Department of Neurosurgery, Kyoto University Graduate School of Medicine, 54 Shogoin-Kawaharacho, Sakyo-ku, Kyoto 606-8507, Japan. Email ishii@kuhp.kyoto-u.ac.jp
Supplemental Material is available at https://www.ahajournals.org/doi/suppl/10.1161/STROKEAHA.122.042043.
For Sources of Funding and Disclosures, see page 1635.

Stroke is available at www.ahajournals.org/journal/str

Nonstandard Abbreviations and Acronyms

αSMA	alpha-smooth muscle actin
CoCr-FD	flow diverter composed of cobalt-chromium and platinum-tungsten
FD	flow diverter
Mw	weight average molecular weight
OCT	optical coherence tomography
PLLA-FD	flow diverter made of poly (L-lactic acid)

have already reached the expected level of success as a device concept.

On the contrary, the placement of permanent metallic FDs is associated with several issues. First, inadequate duration of antiplatelet medication carries the risk of ischemic stroke. Second, when an FD-treated aneurysm recurs, the only endovascular retreatment option is to place an overlapping FD without changing the strategy. Third, FD coverage of any branch vessels near the aneurysm makes the approach impossible. Fourth, FDs cause artifacts on postoperative imaging. These problems could be solved by devices that bioabsorb after aneurysm healing.

Bioresorbable polymers have been used to construct bioresorbable coronary scaffolds with Conformité Européene marking.[7,8] Wang et al[9] first developed a semi-bioresorbable polyglycolic acid FD. We first reported the feasibility of completely bioresorbable poly (L-lactic acid) FD (PLLA-FD) in a preclinical study.[10] Since then, Jamshidi et al[11] have reported preliminary safety data regarding the implantation of a self-expandable PLLA-FD in the rabbit aorta, and the flow diversion behavior of a novel bioresorbable FD has been reported by Muram et al.[12] However, no study has yet compared bioresorbable polymer and metallic FDs. Biological reactions associated with the degradation of bioresorbable materials need to be compared with those of metallic materials. Since our previous report,[10] we have improved the PLLA-FD prototype; now, it is structurally similar to commercial metal FD and has self-expanding properties. In this study, we report its physical properties, bioresorbability, efficacy, and biological responses and compare it with a metallic FD composed of cobalt-chromium and platinum-tungsten (CoCr-FD) in a rabbit model.

METHODS

The data that support the findings of this study are available from the corresponding author upon reasonable request.

FD Design and Mechanical Testing

Bioresorbable medical-grade PLLA (BMG, Kyoto, Japan) with a weight average molecular weight (Mw) of 220 000 g/mol was used as the PLLA-FD material. PLLA was processed into fine fibers by a melt-spinning method. The PLLA-FD was designed as a braided structure with 48 PLLA fibers (inner diameter, 4 mm; length, 10–15 mm; Figure 1A). After annealing and cutting, 3 radiopaque gold markers were attached 1 mm inside each end. The CoCr-FD was braided with 36 cobalt-chromium and 12 platinum-tungsten wires to have identical inner diameter and length as PLLA-FD (Figure 1B). Mechanical performance testing was conducted on PLLA and CoCr wires to evaluate tensile strength, tensile modulus, and elongation rate at break (n=6 per group). Assessments of porosity and pore density (n=4 per group) were performed (see the Supplemental Methods for details). Radial force testing was performed on the PLLA-FD, CoCr-FD, and the initial prototype PLLA-FD we have reported previously.[10]

In Vitro Degradation Testing

To determine the status of the PLLA-FD during the period required for aneurysm healing (real-time degradation test), samples were assessed on months 3, 6, 9, 12, 15, and 18. Gel permeation chromatography assessing Mw and number average molecular weight and radial force testing were performed. To predict when the PLLA-FD bioabsorbes (accelerated degradation test), Gel permeation chromatography was performed on days 3, 6, 9, 12, 15, and 18. Detailed information is described in the Supplemental Methods.

In Vivo Animal Experiments

Aneurysm Construction

The animal study protocol was approved by the Institutional Animal Care Committee of the Kyoto University Graduate School of Medicine (Med Kyo 20253, 21592). Elastase-induced aneurysms were created at the origin of the right common carotid artery in 36 female New Zealand white rabbits (2.6–3 kg; KITAYAMA LABES, Ina, Japan) as described in a previous study.[13] At least 3 weeks were allowed for aneurysm maturation.

FD Implantation

Oral aspirin (30 mg/day) and clopidogrel (30 mg/day) were initiated 1 week before FD implantation. In each rabbit, the same type of FD in the preplanned order was implanted into the right subclavian artery and the abdominal aorta (30 CoCr-FDs in 15 rabbits and 42 PLLA-FDs in 21 rabbits). Detailed information on the procedure of FD implantation is described in the Supplemental Methods. The FDs were deployed proximal to the origin of the right vertebral artery to cover the aneurysm neck and in the abdominal aorta to cover a lumbar artery ostium. For the CoCr-FD, angioplasty was performed only when FD malapposition was suspected. Angioplasty was not used with the PLLA-FD. Aspirin and clopidogrel were continued postoperatively until animal sacrifice.

Specimen Retrieval and Sacrifice

At 3, 6, and 12 months, PLLA-FD rabbits (n=7) and CoCr-FD rabbits (n=5) were anesthetized to perform DSA and optical coherence tomography (OCT; ILUMIEN OPTIS; Abbott Vascular, Santa Clara, CA) at the FD implantation site via a left femoral artery 5F sheath. After evaluation, the rabbits were euthanized. Detailed information on specimen retrieval is described in the Supplemental Methods.

 Stroke. 2023;54:1627–1635. DOI: 10.1161/STROKEAHA.122.042043

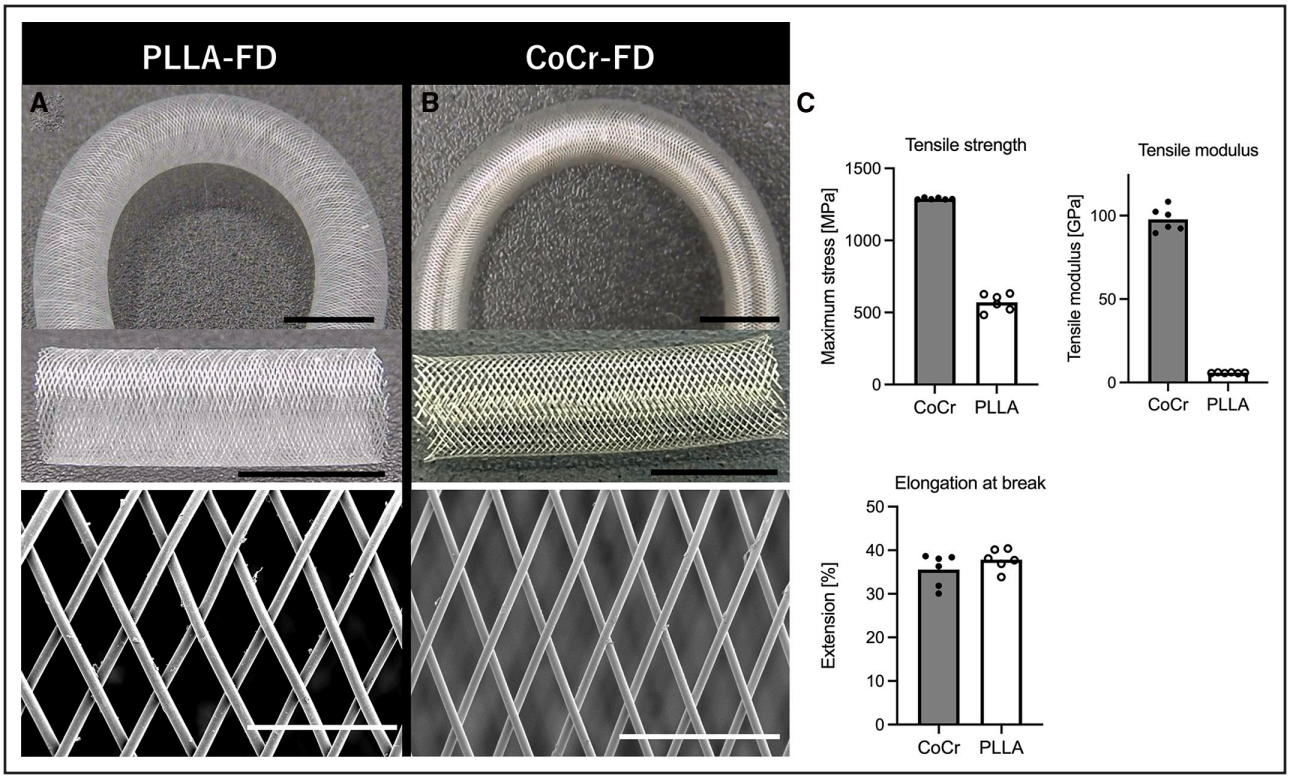

Figure 1. Structure of the 2 types of flow diverters and mechanical properties of the constituent wires.
A, Photographs of the poly (L-lactic acid) flow diverter (PLLA-FD) constructed of 48 fine PLLA fibers (**top**) and scanning electron microscope (SEM) image of the PLLA-FD showing 60% mean porosity and 20 mean pores per mm^2 (**bottom**). **B**, Photographs of the metallic flow diverter constructed of 36 cobalt-chromium and 12 platinum-tungsten wires (CoCr-FD; **top**) and SEM image of the CoCr-FD showing 68% mean porosity and 21 mean pores per mm^2 (**bottom**). Black bars represent 5 mm, and white bars represent 500 μm. **C**, Mean values of tensile strength, tensile modulus, and elongation rate for cobalt-chromium and PLLA wires. Dot plots show the value for each wire (n=6 per group).

Histopathological and Immunohistochemistry Processing

For the aneurysm sample, a cross-section was cut at the aneurysm neck. The abdominal aorta sample was divided into 3 portions (proximal, branch including, and distal). The sections were stained with hematoxylin and eosin, Elastica van Gieson, and Masson trichrome. The primary antibodies were mouse αSMA (alpha-smooth muscle actin) monoclonal antibody, and mouse CD68 monoclonal antibody. Then, the samples were incubated with secondary antibodies. Detailed information is described in the Supplemental Methods.

Tissue Processing for Scanning Electron Microscopy

The details of processing for scanning electron microscopy are shown in the Supplemental Methods.

Data Analysis

Angiographic and OCT Evaluation

Aneurysm size (width, height, and neck) was confirmed on DSA imaging before FD implantation. The degree of aneurysm occlusion (body filling, neck remnant, and complete occlusion) was evaluated by DSA at the time of sacrifice. The patency of the lumbar artery covered by the FD (patent or occluded) was assessed by DSA and OCT. Thrombus formation inside the FD and vessel wall apposition of the FD were evaluated by OCT. FD malapposition was defined as >200 μm between the FD and vessel wall. The wall apposition rate was calculated using the following formula: [1−(FD malapposition length/FD total length in the vessel)]×100%. OCT image analyses were performed using the Offline Review Workstation (Abbott Vascular). Two endovascular specialists independently evaluated all imaging studies in a blinded fashion. In case of discrepancies in semiquantitative or qualitative assessment, the worse rating was used. The mean value was calculated for quantitative measurement.

Histopathological Analysis

Neointimal thickness was measured at 8 points located radially from the center of the vessel on Masson trichrome–stained sections of the abdominal aorta. Neointimal thickness was defined as the distance from the original internal elastic lamina to the luminal border. The mean value was calculated for each section. The composition of the neointima was examined by evaluating elastic fibers with Elastica van Gieson staining (deep purple), collagen fibers with Masson trichrome staining (blue), and smooth muscle with a positive αSMA reaction by immunostaining. The details of how the composition rate was calculated are shown in the Supplemental Methods and figure legends. Within the neointima, CD68-positive cells were counted to evaluate local inflammation. When sections were of insufficient quality or stained, or had FD malapposition as defined above, they were excluded. Each measurement was performed in a blinded manner.

Statistical Analysis

Statistical analyses were performed using JMP Pro 16 (SAS Institute, Inc, Cary, NC) or Prism 9 (GraphPad Software,

San Diego, CA). Continuous data were compared using the unpaired 2-tailed *t* test, Mann-Whitney *U* test, 1-way ANOVA, or the Kruskal-Wallis test. Categorical data were compared using Fisher exact test. $P<0.05$ was considered significant.

RESULTS

Evaluation of Physical Properties of Materials and FDs

For the CoCr and PLLA wires (n=6 per group), mean diameter was 30 μm (range, 30.0–30.0) and 41.7 μm (range, 41.0–42.0). Although tensile strength and tensile modulus differed considerably, elongation at break was comparable (Figure 1C). Mean porosity and mean pore density of the PLLA-FD (n=4) was 60% (range, 56%–63%) and 20 pores per mm^2 (range, 18–23), respectively. Corresponding values of the CoCr-FD (n=4) were 68% (range, 66%–70%) and 21 pores per mm^2 (range, 20–22). On radial force testing, 37% deformation occurred at 0.3 N for PLLA-FD. The strength of the new PLLA-FD was superior to that of the initial PLLA-FD prototype[10]; mean strength calculated on the basis of the change rate was 227% (range, 166%–288%). Mean strength of PLLA-FD compared with CoCr-FD was 99% (range, 78%–118%; Figure 2A).

Degradation Test

Based on the Gel permeation chromatography analysis of the PLLA-FD in the real-time degradation test, the control Mw was 213000 g/mol, which decreased to 62600 g/mol (29%) at 18 months. The control number average molecular weight was 119000 g/mol, which decreased to 13700 g/mol (12%) at 18 months. Mw/number average molecular weight increased from 1.79 (control) to 4.56 at 18 months, reflecting the variation in molecular weight distribution owing to polymer degradation (Figure 2B). The shape of the FD was intact at 18 months. In the accelerated degradation test, the control Mw was 231000 g/mol, which decreased to 15700 g/mol (6.8%) at 18 days (Figure 2C). The FD sample on 18 days lost its stent shape when lightly grasped with forceps. In the radial force test, strength gradually decreased during the degradation process to 44.3% (mean; range, 30.9%–59.7%) of the control sample at 18 months (Figure 2A). The in vivo results are shown in Figure S1.

Angiographic and OCT Outcomes

Angiographic and OCT outcomes are summarized in Table S1, Figures 3A through 3F and 4A through 4C, and Figure S2. Aneurysm size did not significantly differ between the CoCr-FD and PLLA-FD groups with respect to width, height, or neck. The proportion of aneurysms exhibiting either a neck remnant or complete occlusion did not significantly differ between the groups overall (47% and 57%, respectively; $P=0.7360$) or at any time point. However, the complete occlusion rate was significantly higher in the PLLA-FD group (48% versus 13%;

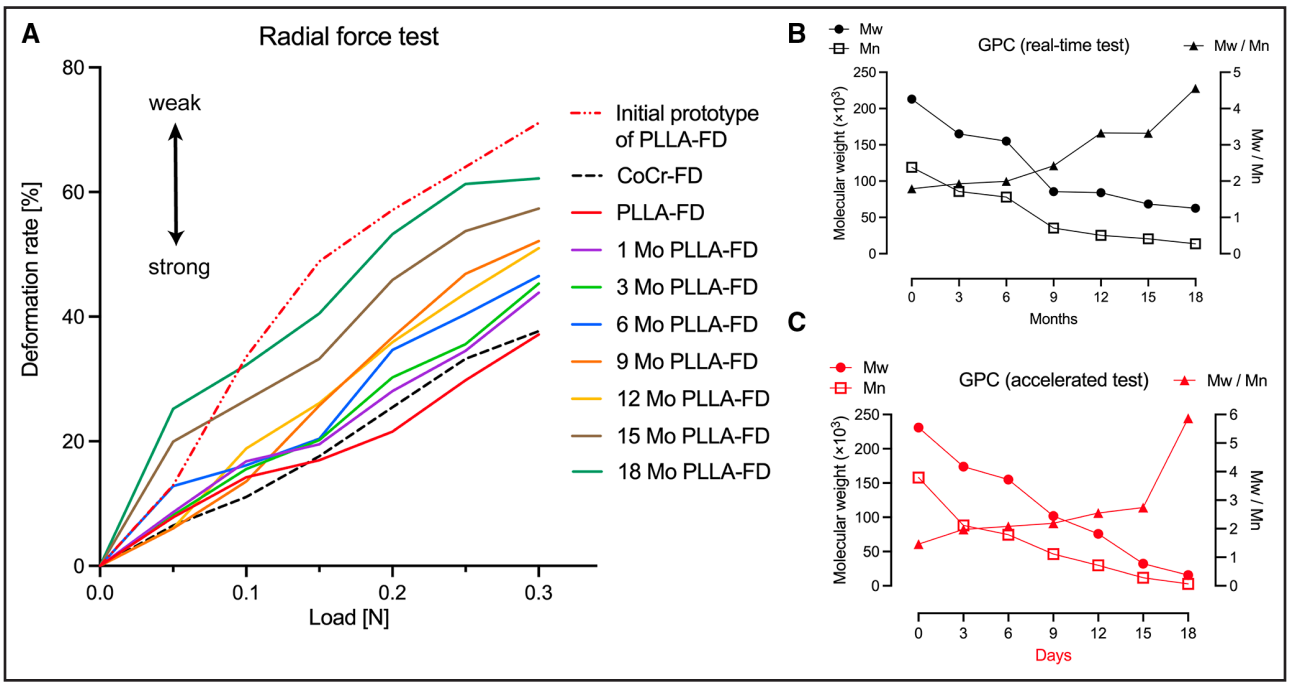

Figure 2. Qualitative variations in the poly (L-lactic acid) flow diverter (PLLA-FD) over time.
A, Results of radial force testing in the PLLA-FD, cobalt-chromium and platinum-tungsten flow diverter (CoCr-FD), initial PLLA-FD prototype, and PLLA-FD after 1, 3, 6, 9, 12, 15, and 18 mo of degradation. **B**, Results of gel permeation chromatography (GPC) in vitro real-time degradation test for PLLA. At 18 mo, weight average molecular weight (Mw) decreased by 71% and number average molecular weight (Mn) decreased by 88%. **C**, Results of GPC in vitro accelerated degradation test for PLLA. Mw decreased by 93% and Mn by 98% at 18 d.

 Stroke. 2023;54:1627–1635. DOI: 10.1161/STROKEAHA.122.042043

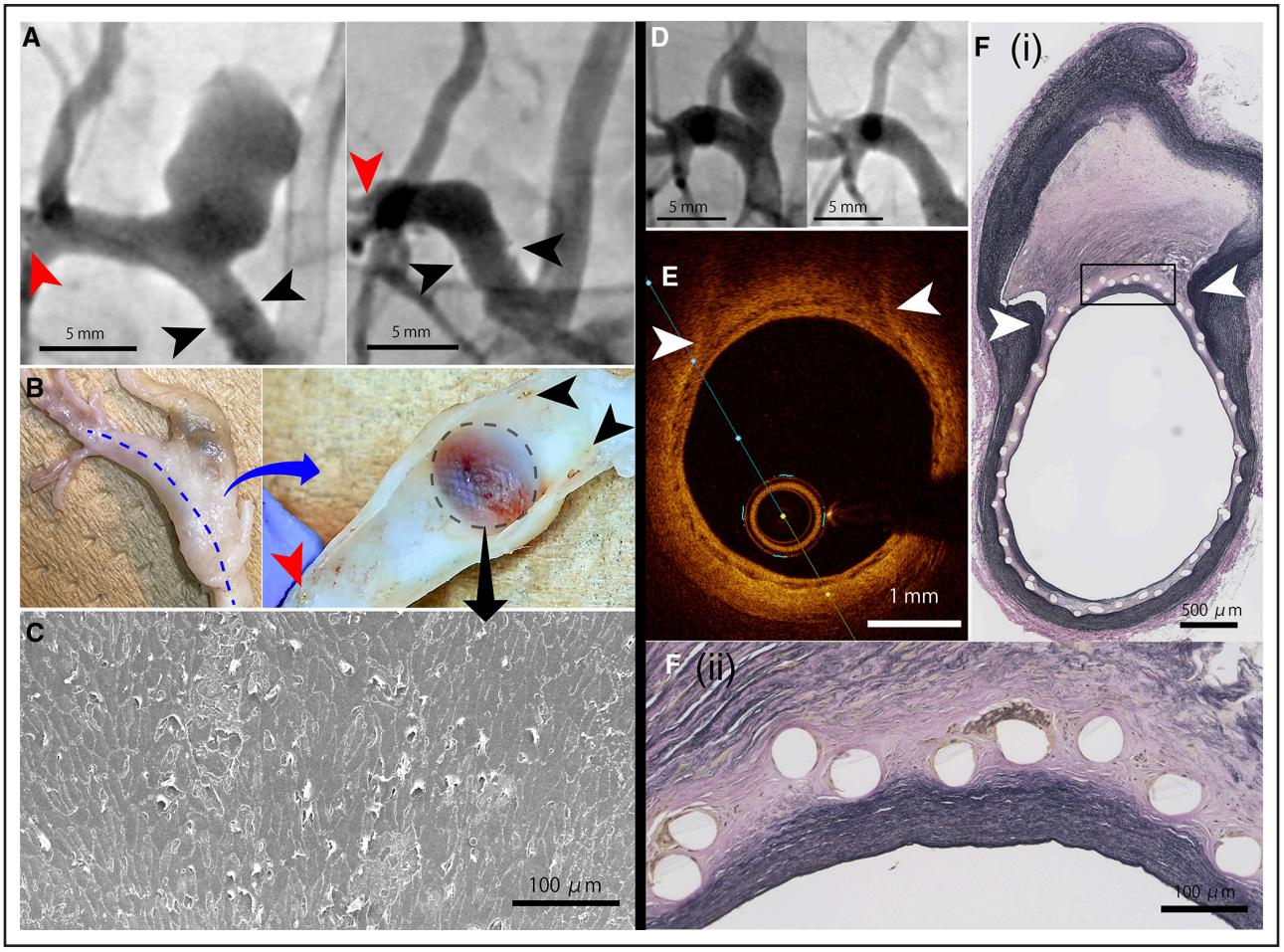

Figure 3. Variations after poly (L-lactic acid) flow diverter (PLLA-FD) implantation at aneurysm site.
A through **C**, Results in 1 rabbit sacrificed 3 mo after PLLA-FD placement. **A**, Angiographic images of the aneurysm before and 3 mo after placement. **B**, Photograph of a specimen taken after trimming (**left**). The blue dotted line represents the cut line for the right photograph. The right photograph was inside the vessel in which the PLLA-FD was implanted. The black dotted line delineates the area of the aneurysm ostium. Neointima grew along the PLLA-FD scaffold and completely occluded the ostium. The red and black arrowheads in **A** and **B** indicate the distal and proximal radiopaque markers, respectively. **C**, Scanning electron microscopy image of the occluded aneurysm ostium. Endothelial cells were observed in the surface layer. **D** through **F**, Results in 1 rabbit sacrificed 3 mo after PLLA-FD placement. **D**, Angiographic images of the aneurysm before and 3 mo after placement. **E**, Cross-sectional optical coherence tomography image capturing the ostium of the occluded aneurysm. **F(i)**, Histological image (Elastica van Gieson staining) of a cross-section of the occluded aneurysm and **F(ii)** enlarged image of the black square in **F(i)**. The aneurysmal occlusion was stabilized from the inside by a monolayer of endothelium, a layer of elastic fibers, and a layer of collagen fibers with strut components. Inflammatory cells are observed around some of the strut components. The white arrowheads in **E** and **F(i)** indicate both ends of the aneurysm neck.

P=0.0399). Occlusion of a covered lumbar artery and thrombus formation within the FD was not identified in either group. The median wall apposition rate did not differ between the 2 groups.

Histopathological Outcomes

The neointima was significantly thicker in the PLLA-FD group than the CoCr-FD group at 3 months (*P*<0.0001) and 6 months (*P*<0.0001); however, neointimal thickness decreased with time in the PLLA-FD group. At 12 months, mean thickness did not significantly differ between the groups (59 versus 66 μm; *P*=0.0973; Figure 4D through 4E; Figure S3). CD68 immunoreactivity within the neointima was significantly higher in the PLLA-FD group at 3 months (*P*=0.0041), 6 months (*P*=0.0489), and 12 months (*P*=0.0383) than in the CoCr-FD group. CD68 immunoreactivity did not significantly differ between time points in the PLLA-FD group (*P*=0.9866; Figure 5A). CD68-positive cells were observed only in the periphery of the struts. No granulation formation was observed. Neointimal composition is summarized in Figure 5B through 5F. The PLLA-FD group had significantly more collagen fibers (*P*=0.0030) and significantly fewer elastic fibers (*P*<0.0001) and smooth muscle cells (*P*=0.0033) than the CoCr-FD group. In particular, the neointima in the PLLA-FD group contained significantly more collagen fibers than elastin fibers (mean collagen/elastin ratio, 1.565 [95% CI, 1.335–1.794]). Nine of the 11 samples in the CoCr-FD

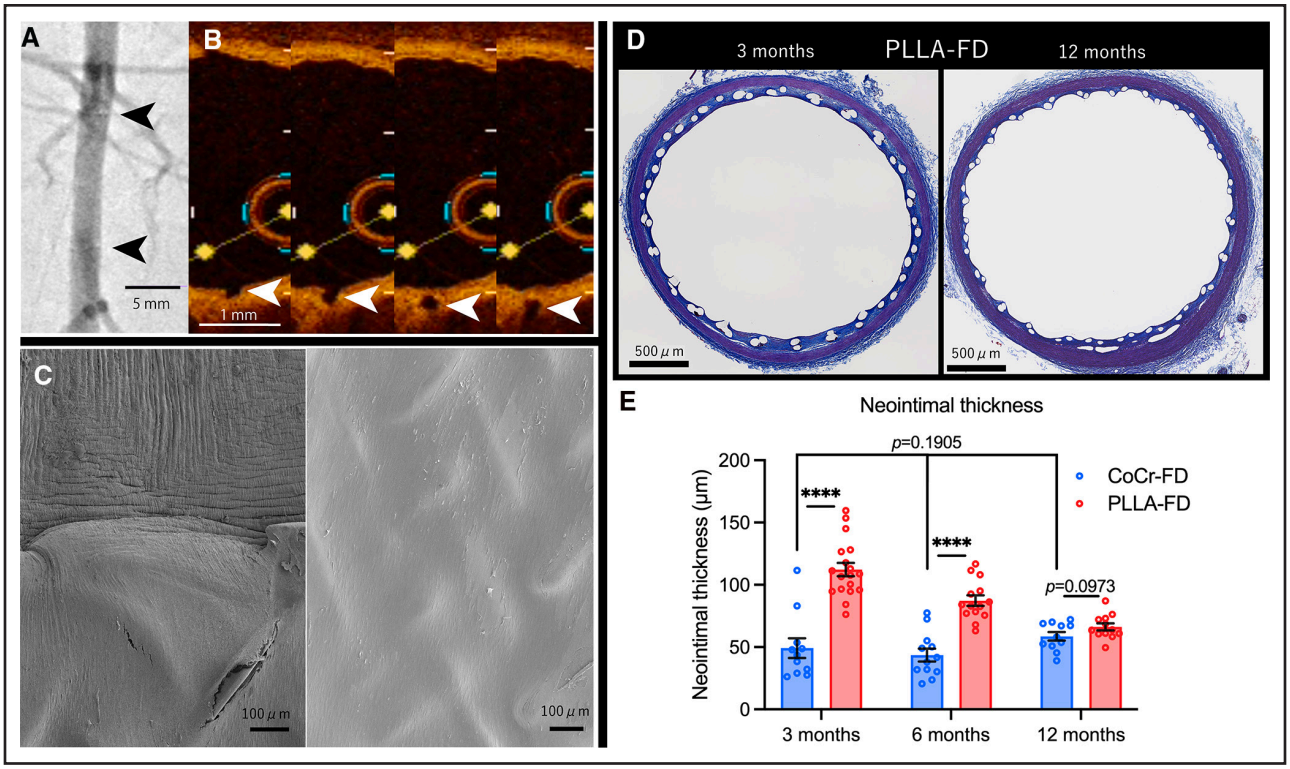

Figure 4. Variations after flow diverter implantation at the abdominal aorta.
A and **B**, Results from 1 rabbit sacrificed 12 mo after poly (L-lactic acid) flow diverter (PLLA-FD) placement. **A**, Angiographic images before sacrifice. The black arrowheads indicate the radiopaque markers. **B**, Four consecutive optical coherence tomography images showed patency of a branch vessel ≈180 μm in diameter (white arrowhead). **C**, Scanning electron microscope images of the abdominal aorta containing the PLLA-FD in 1 rabbit sacrificed 3 mo after implantation. Neointima covered the edge of the PLLA-FD and smoothly transitioned from the normal vessel wall (**left**). The PLLA-FD scaffold was entirely covered with neointima at 3 mo (**right**). **D**, Histological images (Masson trichrome staining) of a cross-section of the abdominal aorta and PLLA-FD. Specimen from a rabbit sacrificed at 3 mo (**left**) and 12 mo (**right**). **E**, Dot plots show mean neointimal thickness per section (n=11, 18, 12,14, 11, and 12 sections; 4, 6, 4, 6, 4, and 6 rabbits, respectively. ****P<0.0001, unpaired 2-tailed t test, 1-way ANOVA). Values represent means±SE.

group showed the opposite, although significance could not be demonstrated (mean collagen/elastin ratio, 0.8664 [95% CI, 0.6693–1.063]). The difference in this ratio between 2 groups was significant at 6 months (P=0.0310) and 12 months (P=0.0176), although not at 3 months (P=0.0523).

DISCUSSION

The Absorb BVS (Abbott Vascular), the first bioresorbable polymer stent approved by the US Food and Drug Administration for use in coronary arteries, had a critical problem with thrombus formation.[14] However, with the maturation of procedural strategies for bioresorbable stents, such as thorough vessel wall apposition, other bioresorbable coronary stents have solved the problem.[7,8,15] We developed a bioresorbable FD made entirely of PLLA and have previously reported a pilot study.[10] However, the initial prototype consisted of 16 braided pairs of 3 PLLA wires and required angioplasty. In addition, its structure and performance were severely inferior to that of commercially available metal FDs. Furthermore, because it degraded rapidly, it did not maintain structure for the period necessary for aneurysm occlusion. Therefore, we made several PLLA-FD modifications for this study. These modifications have resulted in 3 improvements. First, the structure of PLLA-FD approached the porosity (65%–70%) and pore density (>18 pores per mm^2) that are considered ideal for an FD.[1,16] Second, the radial force was twice that of the initial prototype PLLA-FD (Figure 2A),[10] allowing the PLLA-FD to self-expand. A radial force of 0.3 N caused 37% deformation in our study, which demonstrates adequate strength similar to that of the FD of PLLA reported by Jamshidi et al[11] (0.45 N to reach 50% deformation). Third, the polymer bioabsorption period was prolonged and structure was maintained for 12 months, which appears to be the minimum required period based on previous clinical studies.[17] The PLLA-FD structure was maintained at 18 months (Mw, 62 600 g/mol) in the real-time degradation test but not at 15 700 g/mol of Mw in the accelerated degradation test. The correlation between polymer molecular weight and physical properties is consistent with previous reports.[18–20] These results suggest that FD degradation and absorption would occur around 24 months in real time. As a result of these 3 improvements, the complete

 Stroke. 2023;54:1627–1635. DOI: 10.1161/STROKEAHA.122.042043

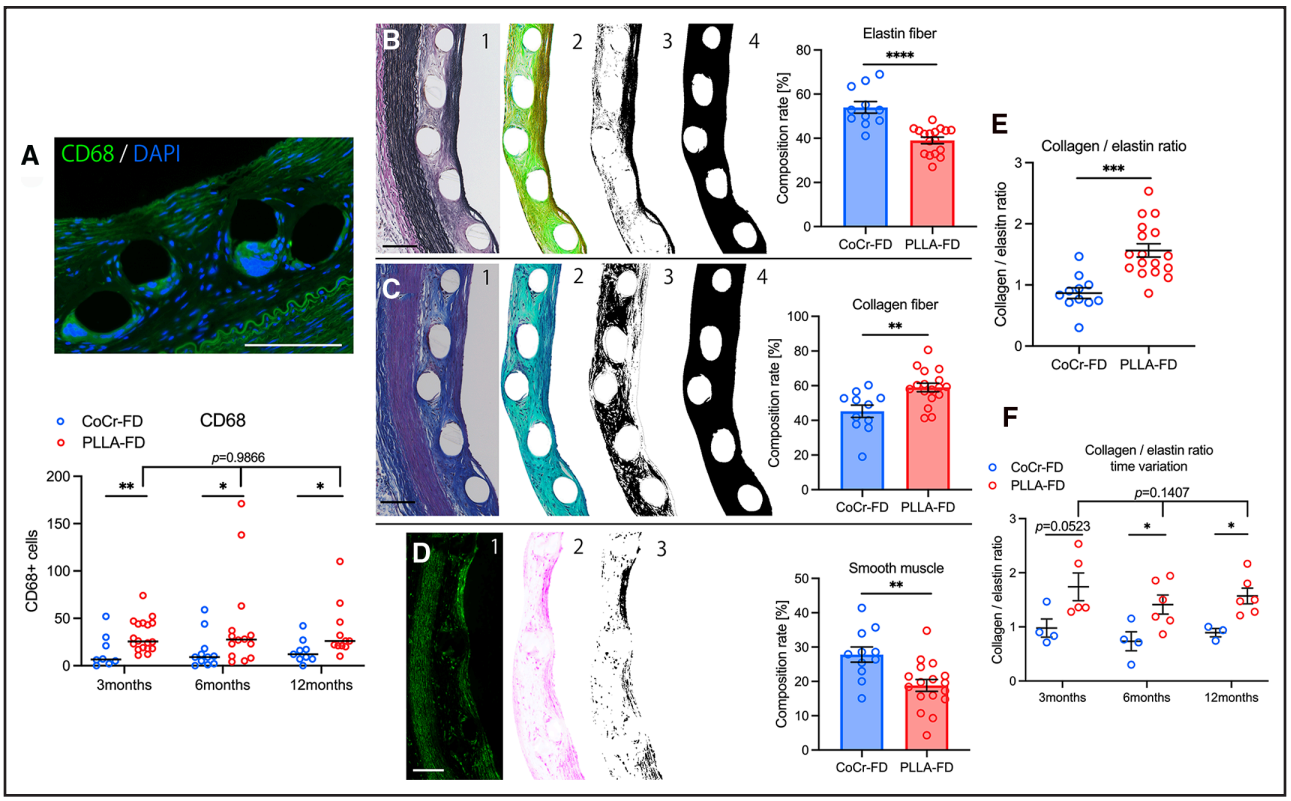

Figure 5. Differences between groups regarding local inflammation and vessel remodeling after flow diverter implantation. **A**, Representative image of CD68 immunoreactivity in the neointima. Dot plots show CD68-positive cells per section (n=9, 18, 11, 14, 8, and 11 sections; 4, 6, 4, 6, 3, and 6 rabbits, respectively. ***P*<0.01, **P*< 0.05, Mann-Whitney *U* test and Kruskal-Wallis test). Values represent medians. **B**, Imaging process for calculating the percentage of elastin fiber composition within the neointima: (B-1) image of specimen stained with Elastica van Gieson; (B-2) image-adjusted hue and saturation under all the same conditions to clarify the color of elastin fibers from other colors after trimming just the neointima using Photoshop; (B-3) image converted to binary data using the ImageJ software; (B-4) image of the entire neointima obtained after optimizing the threshold of image B-2 under all the same conditions. **C**, Imaging process for calculating the percentage of collagen fiber composition within the neointima: (C-1) image of specimen stained with Masson trichrome; (C-2) image-adjusted hue and saturation under all the same conditions to clarify the color of collagen fibers from other colors after trimming just the neointima using Photoshop; (C-3) image converted to inverted binary data using the ImageJ software; (C-4) image of the entire neointima after optimizing the threshold of image C-2 under all the same conditions. **D**, Imaging process for calculating the percentage of smooth muscle composition within the neointima: (D-1) image of αSMA (alpha-smooth muscle actin)-positive cells; (D-2) inverted image of image D-1 after trimming just the neointima using Photoshop; (D-3) image converted to binary data. The area of neointima was calculated as the mean of the black areas in B-4 and C-4. The elastin fiber, collagen fiber, and smooth muscle composition rates were calculated as [(black area of B-3)/(area of neointima)]×100%, [(black area of C-3)/(area of neointima)]×100%, and [(black area of D-3)/(area of neointima)]×100%, respectively. Dot plots of the elastin fiber, collagen fiber, and smooth muscle composition rates and collagen fiber/elastin fiber ratio overall and (**E**) over time (**F**) in the cobalt-chromium and platinum-tungsten flow diverter (CoCr-FD) and poly (L-lactic acid) flow diverter (PLLA-FD) groups (n=11 and 17 sections; 11 and 17 rabbits, respectively. *****P*<0.0001, ****P*<0.001, ***P*<0.01, **P*<0.05, unpaired 2-tailed *t* test and 1-way ANOVA). Values represent means±SE. Bars, 100 μm.

aneurysm occlusion rate in this study (48%) was twice the rate reported in our previous study (24%)[10] and comparable to the 53% rate reported for the first-generation pipeline embolization device during development.[21] Although the radial force of the PLLA-FD and CoCr-FD were comparable, the PLLA-FD was associated with a significantly higher rate of complete occlusion. These results suggest that PLLA is feasible as a material for FD construction. However, the second-generation pipeline embolization device clinically applied was associated with a 93% complete occlusion rate in an animal study.[22] Therefore, further improvements in the PLLA-FD are needed for clinical application.

In our previous study, the incidence of thrombus formation within the PLLA scaffold was 1.8% at 3 months and none after 6 months.[10] In this study, OCT showed no thrombus formation within the FD, possibly because of improved vessel wall apposition and a braided structure, as shown in a previous report on coronary stents.[23] As with bioresorbable coronary stents, thrombosis may not be a major problem in sufficient wall apposition of PLLA-FD.[7,8,15] Neointimal proliferation may cause lumen area stenosis; however, in this study, neointimal thickness in the PLLA-FD group decreased over time and was not significantly different from that of the CoCr-FD group at 12 months (Figure 4E). This result is consistent with our previous study in which neointimal thickness peaked at 3 months.[10] Otsuka et al[24] reported that neointimal thickening was greater with bioresorbable polymer stents than with bare cobalt-chromium stents over 3.5 years in a porcine coronary

artery. Sadasivan et al[16] reported that lower porosity and lower pore density are associated with neointimal thickening. These results suggested that the initial difference in neointimal thickness between the 2 groups might have been due to the differences in material or pore structure and due to differences in strut thickness. Unlike the process in coronary stents, the lack of significant differences in thickness after 12 months between the 2 groups may be attributed to the thinner struts of FD. In fact, a new generation of coronary stent with ultrathin struts is also expected to decrease neointimal proliferation.[25] However, local inflammation as shown by CD68 was significantly higher in the PLLA-FD group than the CoCr-FD group at all observation points and did not decrease over time. Thus, the course of neointimal thickness differences did not correlate with the course of inflammation differences. Otsuka et al[24] also reported that inflammation was significantly higher for bioresorbable polymer coronary stents than for cobalt-chromium coronary stents for >3 years. In the present study, CD68-positive cells were observed only around the strut, which may represent an ongoing inflammatory response to the lactic acid produced by hydrolysis of the PLLA. Therefore, such findings may persist for as long as the resorption process continues. Collagen fibers predominated over elastic fibers in the neointima in the PLLA-FD group at all time points and vice versa in the CoCr-FD group (Figure 5F). The differences in the composition of the extracellular matrix might be due to differences in inflammation because of a similar process. An increased collagen/elastin ratio is not ideal for arterial vascular remodeling because it decreased vascular extensibility,[26] but they might be more biocompatible than a permanent implant remaining in the vessel. The reduction in neointimal thickness while maintaining the composition needs to be verified, and long-term and immunohistological evaluations will be necessary in the future. Consequently, we identified no obvious morphological or pathological problems with the PLLA-FD in this study.

Bioresorbable coronary scaffolds with polymer or magnesium have been applied in clinical practice.[27] Oliver et al[28] reported that metals such as iron or magnesium would be ideal for the material of bioresorbable FDs in terms of mechanical strength and biocompatibility. However, the number of reports regarding bioresorbable FD is limited.[9–12] The reason for this lack of reports is that achieving the ideal FD structure is challenging owing to its inferior strength or difficulty in adjusting the absorption period. Bioresorbable FDs of any material will continue to be developed as a solution to the problems associated with permanent metallic ones.

Limitations

This study has several limitations. First, the aneurysm healing rate in the CoCr-FD group was lower than that reported in previous studies.[16,22] A post-project survey showed that the radial force of the CoCr-FD increased >2.35× by changing the annealing conditions. Vessel wall apposition is the most important factor in aneurysm occlusion.[29] Therefore, insufficient radial force due to inadequate annealing conditions may have resulted in incomplete FD apposition and a lower aneurysm healing rate of CoCr-FD. Second, in the present study, visibility was limited to radiopaque markers at both ends because we aimed to create FDs with uniformity of structure using only pure PLLA. This may have resulted in insufficient apposition of the PLLA-FD to the vessel wall. In clinical applications, another solution is required, such as replacing the wire with a visible wire as reported by Jamshidi et al.[11] Third, OCT imaging at FD implantation, which confirmed FD apposition to the vessel wall, was missing. This lack of imaging and insufficient radial force may have led to a low cure rate in the CoCr-FD group. In addition, the PLLA-FD group may have achieved a higher cure rate with OCT imaging, which can compensate for the problem of radiopacity. Fourth, the potential problem of fragmentation in bioresorbable materials was not adequately verified. Since all lumbar arteries were patent and the struts of the FD floating on the ostium of the branching vessel were covered with endothelial cells (Figure S4), it cannot be concluded that fragmentation is an inevitable problem. However, if the FD had been implanted in the aorta, including the renal artery bifurcation, a detailed examination of the kidney could have provided more information about the potential fragmentation. Nevertheless, in this study, the FD did not cover renal artery bifurcation. Fifth, the FD was not placed distal to the origin of the right vertebral artery to avoid a diameter mismatch between the vessel and the FD. Therefore, the performance of the FD in a vessel <2 mm was not assessed. Further studies are required to investigate the performance of the FD in a small vessel, particularly considering the early-stage neointimal thickening observed with the PLLA-FD.

Conclusions

The PLLA-FD is feasible for the treatment of intracranial aneurysms and was as effective as the CoCr-FD in this study. No morphological and pathological adverse events were observed with bioresorbable PLLA-FD over a 1-year period. There continues to be a need to improve healing rate by increasing radial force and achieving radiographic visibility.

ARTICLE INFORMATION

Received November 18, 2022; final revision received March 11, 2023; accepted March 30, 2023.

Affiliations

Department of Neurosurgery, Kyoto University Graduate School of Medicine, Japan (N.S., A.I., H.N., R.A., M.O., Y.A., H.T., S.M.). Department of Biobased Materials Science, Kyoto Institute of Technology, Japan (S.Y., S.S.). RADIS Lab, Research in Cerebral Vascular Diseases, Division of Neurosurgery, St. Michael's Hospital, Toronto, Ontario, Canada (H.N.).

Acknowledgments

We thank Kyoto Medical Planning (Kyoto, Japan) for its generous donation of the experimental-related device and Dr Shin Watanabe of the Department of Cardiovascular Medicine of Kyoto University Hospital for his assistance with the optical coherence tomography workstation. We also thank the Institute of Laboratory Animals, Graduate School of Medicine, at the Kyoto University for animal management and Edanz (https://jp.edanz.com/ac) for English editing. Electron microscopy support was provided by the Division of Electron Microscopic Study, Center for Anatomical Studies, Graduate School of Medicine, at the Kyoto University.

Sources of Funding

This work was supported by JSPS KAKENHI (Grants-in-Aid for scientific research from Japan Society for the Promotion of Science) grant number 22K09255.

Disclosures

None.

Supplemental Material

Supplemental Methods
Table S1
Figures S1–S4

REFERENCES

1. Dandapat S, Mendez-Ruiz A, Martínez-Galdámez M, Macho J, Derakhshani S, Foa Torres G, Pereira VM, Arat A, Wakhloo AK, Ortega-Gutierrez S. Review of current intracranial aneurysm flow diversion technology and clinical use. *J Neurointerv Surg*. 2021;13:54–62. doi: 10.1136/neurintsurg-2020-015877
2. Brinjikji W, Murad MH, Lanzino G, Cloft HJ, Kallmes DF. Endovascular treatment of intracranial aneurysms with flow diverters: a meta-analysis. *Stroke*. 2013;44:442–447. doi: 10.1161/STROKEAHA.112.678151
3. Zhou G, Su M, Zhu YQ, Li MH. Efficacy of flow-diverting devices for cerebral aneurysms: a systematic review and meta-analysis. *World Neurosurg*. 2016;85:252–262. doi: 10.1016/j.wneu.2015.09.088
4. Hanel RA, Kallmes DF, Lopes DK, Nelson PK, Siddiqui A, Jabbour P, Pereira VM, Szikora István I, Zaidat OO, Bettegowda C, et al. Prospective study on embolization of intracranial aneurysms with the pipeline device: the PREMIER study 1 year results. *J Neurointerv Surg*. 2020;12:62–66. doi: 10.1136/neurintsurg-2019-015091
5. Killer-Oberpfalzer M, Kocer N, Griessenauer CJ, Janssen H, Engelhorn T, Holtmannspötter M, Buhk JH, Finkenzeller T, Fesl G, Trenkler J, et al. European multicenter study for the evaluation of a dual-layer flow-diverting stent for treatment of wide-neck intracranial aneurysms: the European flow-redirection intraluminal device study. *Am J Neuroradiol*. 2018;39:841–847. doi: 10.3174/ajnr.A5592
6. Fiorella D, Lylyk P, Szikora I, Kelly ME, Albuquerque FC, McDougall CG, Nelson PK. Curative cerebrovascular reconstruction with the pipeline embolization device: the emergence of definitive endovascular therapy for intracranial aneurysms. *J Neurointerv Surg*. 2009;1:56–65. doi: 10.1136/jnis.2009.000083
7. Nef H, Wiebe J, Boeder N, Dörr O, Bauer T, Hauptmann KE, Latib A, Colombo A, Fischer D, Rudolph T, et al. A multicenter post-marketing evaluation of the Elixir DESolve® Novolimus-eluting bioresorbable coronary scaffold system: first results from the DESolve PMCF study. *Catheter Cardiovasc Interv*. 2018;92:1021–1027. doi: 10.1002/ccd.27550
8. Chevalier B, Abizaid A, Carrié D, Frey N, Lutz M, Weber-Albers J, Dudek D, Weng SC, Akodad M, Anderson J, et al. Clinical and angiographic outcomes with a novel radiopaque sirolimus-eluting bioresorbable vascular scaffold: the FANTOM II study. *Circ Cardiovasc Interv*. 2019;12:1–8.
9. Wang K, Yuan S, Zhang X, Liu Q, Zhong Q, Zhang R, Lu P, Li J. Biodegradable flow-diverting device for the treatment of intracranial aneurysm: short-term results of a rabbit experiment. *Neuroradiology*. 2013;55:621–628. doi: 10.1007/s00234-013-1150-0
10. Nishi H, Ishii A, Ono I, Abekura Y, Ikeda H, Arai D, Yamao Y, Okawa M, Kikuchi T, Nakakura A, et al. Biodegradable flow diverter for the treatment of intracranial aneurysms: a pilot study using a rabbit aneurysm model. *J Am Heart Assoc*. 2019;8:1–13.
11. Jamshidi M, Rajabian M, Avery MB, Sundararaj U, Ronsky J, Belanger B, Wong JH, Mitha AP. A novel self-expanding primarily bioabsorbable braided flow-diverting stent for aneurysms: initial safety results. *J Neurointerv Surg*. 2020;12:700–705. doi: 10.1136/neurintsurg-2019-015555
12. Muram S, Corcoran R, Cooke J, Forrester K, Lapins E, Morrish R, Cheema OZA, Goyal M, Eesa M, Fiorella D, et al. Immediate flow-diversion characteristics of a novel primarily bioresorbable flow-diverting stent. *J Neurosurg*. 2022;137:1794–1800. doi: 10.3171/2022.1.JNS212975
13. Altes TA, Cloft HJ, Short JG, Degast A, Do HM, Helm GA, Kallmes DF. Creation of saccular aneurysms in the rabbit: a model suitable for testing endovascular devices. *Am J Roentgenol*. 2000;174:349–354. doi: 10.2214/ajr.174.2.1740349
14. Wykrzykowska JJ, Kraak RP, Hofma SH, van der Schaaf RJ, Arkenbout EK, IJsselmuiden AJ, Elias J, van Dongen IM, Tijssen RYG, Koch KT, et al; AIDA Investigators. Bioresorbable scaffolds versus metallic stents in routine PCI. *N Engl J Med*. 2017;376:2319–2328. doi: 10.1056/NEJMoa1614954
15. Puricel S, Cuculi F, Weissner M, Schmermund A, Jamshidi P, Nyffenegger T, Binder H, Eggebrecht H, Münzel T, Cook S, et al. Bioresorbable coronary scaffold thrombosis: multicenter comprehensive analysis of clinical presentation, mechanisms, and predictors. *J Am Coll Cardiol*. 2016;67:921–931. doi: 10.1016/j.jacc.2015.12.019
16. Sadasivan C, Cesar L, Seong J, Rakian A, Hao Q, Tio FO, Wakhloo AK, Lieber BB. An original flow diversion device for the treatment of intracranial aneurysms: evaluation in the rabbit elastase-induced model. *Stroke*. 2009;40:952–958. doi: 10.1161/STROKEAHA.108.533760
17. Becske T, Brinjikji W, Potts MB, Kallmes DF, Shapiro M, Moran CJ, Levy EI, McDougall CG, Szikora I, Lanzino G, et al. Long-term clinical and angiographic outcomes following pipeline embolization device treatment of complex internal carotid artery aneurysms: five-year results of the pipeline for uncoilable or failed aneurysms trial. *Neurosurgery*. 2017;80:40–48. doi: 10.1093/neuros/nyw014
18. Lunt J. Large-scale production, properties and commercial applications of poly lactic acid polymers. *Polym Degrad Stab*. 1998;59:145–152. doi: 10.1016/s0141-3910(97)00148-1
19. Zhao G, Wang B, Li X, Liu M, Tian Y, Zhang J, Zhang Y, Cheng J, Yang J, Ni Z. Evaluation of poly (L-lactic acid) monofilaments with high mechanical performance in vitro degradation. *J Mater Sci*. 2022;57:6361–6371.
20. Weir NA, Buchanan FJ, Orr JF, Dickson GR. Degradation of poly-L-lactide. Part 1: in vitro and in vivo physiological temperature degradation. *Proc Inst Mech Eng H*. 2004;218:307–319. doi: 10.1243/0954411041932782
21. Kallmes DF, Ding YH, Dai D, Kadirvel R, Lewis DA, Cloft HJ. A new endoluminal, flow-disrupting device for treatment of saccular aneurysms. *Stroke*. 2007;38:2346–2352. doi: 10.1161/STROKEAHA.106.479576
22. Kallmes DF, Ding YH, Dai D, Kadirvel R, Lewis DA, Cloft HJ. A second-generation, endoluminal, flow-disrupting device for treatment of saccular aneurysms. *Am J Neuroradiol*. 2009;30:1153–1158. doi: 10.3174/ajnr.A1530
23. Kolandaivelu K, Swaminathan R, Gibson WJ, Kolachalama VB, Nguyen-Ehrenreich KL, Giddings VL, Coleman L, Wong GK, Edelman ER. Stent thrombogenicity early in high-risk interventional settings is driven by stent design and deployment and protected by polymer-drug coatings. *Circulation*. 2011;123:1400–1409. doi: 10.1161/CIRCULATIONAHA.110.003210
24. Otsuka F, Pacheco E, Perkins LEL, Lane JP, Wang Q, Kamberi M, Frie M, Wang J, Sakakura K, Yahagi K, et al. Long-term safety of an everolimus-eluting bioresorbable vascular scaffold and the cobalt-chromium XIENCE V stent in a porcine coronary artery model. *Circ Cardiovasc Interv*. 2014;7:330–342. doi: 10.1161/CIRCINTERVENTIONS.113.000990
25. Iglesias JF, Heg D, Roffi M, Tüller D, Noble S, Muller O, Moarof I, Cook S, Weilenmann D, Kaiser C, et al. Long-term effect of ultrathin-strut versus thin-strut drug-eluting stents in patients with small vessel coronary artery disease undergoing percutaneous coronary intervention: a subgroup analysis of the BIOSCIENCE randomized trial. *Circ Cardiovasc Interv*. 2019;12:1–10.
26. Basu P, Sen U, Tyagi N, Tyagi SC. Blood flow interplays with elastin: collagen and MMP: TIMP ratios to maintain healthy vascular structure and function. *Vasc Health Risk Manag*. 2010;6:215–228. doi: 10.2147/vhrm.s9472
27. Boeder NF, Dörr O, Koepp T, Blachutzik F, Achenbach S, Elsässer A, Hamm CW, Nef HM. Acute mechanical performance of magmaris vs. DESolve bioresorbable scaffolds in a real-world scenario. *Front Cardiovasc Med*. 2021;8:1–7.
28. Oliver AA, Carlson KD, Bilgin C, Arturo Larco JL, Kadirvel R, Guillory RJ, Dragomir Daescu D, Kallmes DF. Bioresorbable flow diverters for the treatment of intracranial aneurysms: review of current literature and future directions. *J Neurointerv Surg*. 2023;15:178–182. doi: 10.1136/neurintsurg-2022-018941
29. Rouchaud A, Ramana C, Brinjikji W, Ding YH, Dai D, Gunderson T, Cebral J, Kallmes DF, Kadirvel R. Wall apposition is a key factor for aneurysm occlusion after flow diversion: a histologic evaluation in 41 rabbits. *Am J Neuroradiol*. 2016;37:2087–2091. doi: 10.3174/ajnr.A4848